Dendrochronologia 44 (2017) 164–173

Contents lists available at ScienceDirect

Dendrochronologia

journal homepage: www.elsevier.com/locate/dendro

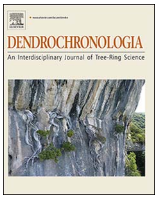

High-elevation inter-site differences in Mount Smolikas tree-ring width data

Lara Klippel[a,*], Paul J. Krusic[b,c], Robert Brandes[d], Claudia Hartl-Meier[a], Valerie Trouet[e], Matthew Meko[e], Jan Esper[a]

[a] Department of Geography, Johannes Gutenberg University, 55099 Mainz, Germany
[b] Department of Geography, University of Cambridge, Cambridge CB2 3EN, United Kingdom
[c] Navarino Environmental Observatory, Messinia, Greece
[d] Department of Geography, Friedrich-Alexander University Erlangen-Nürnberg, 91058 Erlangen, Germany
[e] Laboratory of Tree-Ring Research, University of Arizona, Tucson, AZ 85721, USA

ARTICLE INFO

Keywords:
Pinus heldreichii
Dendroclimatology
Mediterranean climate
Greece
Tree-ring width
Treeline ecotone

ABSTRACT

We present the longest high-elevation tree-ring width dataset in the Mediterranean reaching back to the 6th century CE. The network includes 101 living and 92 relict *Pinus heldreichii* Christ trees from four differently exposed sites in the 2100–2200 m a.s.l. elevation range of Mt. Smolikas in the Pindus Mountains in Greece. Though the sites were all sampled within a distance of < 1 km, inter-site correlations are surprisingly low ($r_{1550–2014} = 0.65–0.87$), indicating site exposure might affect tree-ring formation. We here explore the consequence of exposure differences on the climate signals in an eastern Mediterranean treeline ecotone. Temporally stable growth/climate relationships reveal similar seasonal patterns among the four sites, but differences in signal strength. *P. heldreichii* growth at Mt. Smolikas is significantly controlled by temperature in April ($r_{1951–2014} = 0.33–0.50$) and precipitation in June-July ($r_{1951–2014} = 0.23–0.42$), which emphasizes the overall importance of an early growth onset and subsequent moisture conditions. The association between stem growth and April climate is strongest in the South-facing stand, supporting the significance of higher insolation rates at this thermally privileged site. Strongest summer precipitation signals are found in the NE-facing stand, where trees seem to benefit least from an early growth onset and where reduced meltwater supply may enhance the dependency on early summer precipitation. The significance of spring temperature on tree growth in all four sites constrains the emergence of a distinct summer precipitation signal in the Mt. Smolikas high elevation ecotone. Exploration of the site-specific influences on a new millennium-long tree-ring width dataset is an important step towards an improved understanding of long-term climate variability in the Eastern Mediterranean. Site-related differences in climate sensitivity in the high-elevation tree-ring network at Mt. Smolikas indicate that both temperature and precipitation during different seasons could potentially be reconstructed if distinct site exposures (S versus NE) are considered.

1. Introduction

Tree-ring width (TRW) chronologies are an important proxy for the reconstruction of climate variability over the past millennium (Esper et al., 2016). Information about past climate conditions and their implications for society improve our understanding of natural and anthropogenically driven climate variability (Büntgen et al., 2011). This is crucial in the development of future climate scenarios and the evaluation of potential social and environmental impacts of climate (Esper et al., 2004; Kovats et al., 2014). Continuous improvement of the spatial coverage by millennium-length TRW chronologies is needed to assess climate variability patterns and their association with forcings at regional (Köse et al., 2011; Seftigen et al., 2013; Trouet et al., 2012) and hemispheric scales (D'Arrigo et al., 2006; Esper et al., 2002; Schneider et al., 2015; Stoffel et al., 2015; Wilson et al., 2016).

P. heldreichii Christ (or Bosnian pine) is a Tertiary relict tree species, endemic to the high mountains of the Balkans, and is abundant in northern Greece, western Bulgaria, Bosnia-Herzegovina, and Albania (Brandes, 2007). The species survives in very old stands with individuals of millennial age (Konter et al., 2017) demonstrating the potential of these sites to contribute to high-resolution paleoclimate reconstruction. The wood of *P. heldreichii* is very resinous and consequently resistant to decay and decomposition. This characteristic is beneficial for preserving material from fallen trees, especially in remote areas of the timberline ecotone (Brandes, 2007).

Numerous Bosnian pine chronologies have been developed from

---

[*] Corresponding author.
E-mail address: L.Klippel@geo.uni-mainz.de (L. Klippel).

http://dx.doi.org/10.1016/j.dendro.2017.05.006
Received 3 May 2017; Accepted 29 May 2017
Available online 03 June 2017

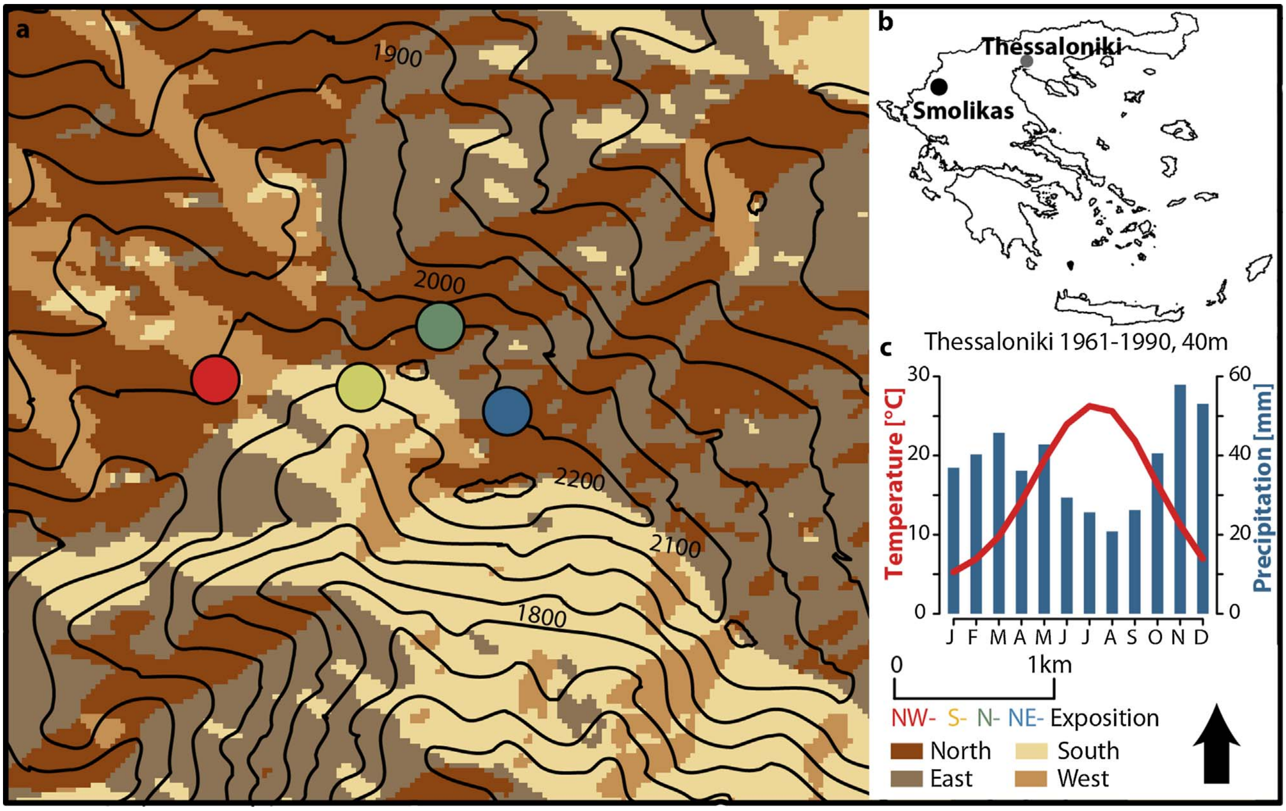

Fig. 1. **a** Contour and site exposure map of the study region and position of the sampling sites; **b** map of Greece indicating the research area and the instrumental station, **c** Climate diagram of the meteorological station in Thessaloniki (40 m a.s.l., 1961–1990).

collections in various areas of the species' range. These extant chronologies have two common features: they are typically very long, and the climate signal from their TRW measurements is weak (maximum $r_{1901-2002} = -0.29$ with June-July temperature in Seim et al. (2012); $r_{1925-2000} = 0.29$ with April Temperature in Todaro et al. (2007); $r_{1934-2004} = 0.38$ with previous August Precipitation, and $r_{1985-1992} = \sim$-0.3 with June temperature in Panayotov et al. (2010)). The species is resistant to a rough mountain climate and can tolerate harsh winters as well as a certain degree of summer drought. Therefore, the existence of the pure, zonal *P. heldreichii*-stands in northern Greece is explained by the seasonal extremes of a low latitude mountain climate (Brandes, 2007).

Theories explaining the low climate sensitivity are diverse and encompass anthropogenic activity, the remoteness of meteorological stations, and mixed climate controls (Panayotov et al., 2010; Seim et al., 2012; Todaro et al., 2007). However, most previous studies did not consider site-specific ecological constraints as influences on climate signals (Holland and Steyn, 1975; Schweingruber, 1996). Near to the Greek border with Albania, Mount Smolikas (2637 m a.s.l.) crowns the mountain range of the northern Pindus mountains at 40°05′N/20°55′E (Fig. 1a and b). The sites in this study are situated around an eastern foothill of Mt. Smolikas and differ in exposure only (Fig. 1b). Slope aspect alters the amount of received solar radiation and length of insolation period, thus creating a range of microclimates on a small spatial scale (Gallardo-Cruz et al., 2009; Hartl-Meier et al., 2014; Hartl-Meier et al., 2015; Holland and Steyn, 1975; Urban et al., 2000). Insolation controls evapotranspiration, soil and air temperature, air humidity, soil moisture, and the duration of the growing period that in turn affects the species composition and biomass production (Måren et al., 2015; Paudel and Vetaas, 2014; Pook and Moore, 1966). In the Mediterranean, south-facing slopes receive the most sunlight, which supports evapotranspiration and results in drought stress for trees, whereas north-facing slopes retrain more humidity and favor growth (Sternberg and Shoshany, 2001).

In this study, we explore the effect of slope exposure on tree growth and the impact on potentially varying climate signals by calibrating the chronologies of four differently exposed, high elevation *P. heldreichii* sites against regional instrumental temperature, precipitation, and drought data. We introduce a preliminary millennium-length TRW dataset and evaluate its potential and limitations for establishing a climate reconstruction.

2. Material and methods

2.1. Geographical settings and sampling design

In northern Greece, *P. heldreichii* is native to the upper oro-mediterranean vegetation zone and appears first at ca. 1.000 m a.s.l. in mixed forests with *Fagus sylvatica* L., *Pinus nigra* J.F. Arnold, and *Abies borisii-regis* Mattf. Between 1.500-2.300 m a.s.l., *P. heldreichii* forms pure stands to the timberline, with dwarfed specimens reaching 2.600 m a.s.l. on Mt. Olympus (Brandes, 2007). The southern distribution limit of the species is near the village Metsovon, in the Pindus mountains, at 39°40′ N. On Mt. Smolikas, the zone of pure *P. heldreichii* stands starts at 1.300-1.500 m a.s.l. and transforms into an open timberline ecotone at 1.900-2.400 m a.s.l. (Brandes, 2007). Anthropogenic impacts are presently constrained to pastoral farming. However, the name Mt. Smolikas, originating from the Slavic word "Smola" (engl. tar), points to a much greater economic importance of the area in the past, when the *P. heldreichii* resins were extracted for tar production (Meiggs, 1982). Geologically the higher areas of the mountain are formed by serpentine, a dry bedrock poor in nutrients, but not karstified or fissured (Hughes et al., 2006; Stevanovic et al., 2003). *P. heldreichii* grows on dry substrate, such as limestone and serpentine rocks.

Between 2011 and 2015, 101 living and 92 dead *P. heldreichii* trees were sampled in this timberline ecotone in 2100–2200 m a.s.l. at four

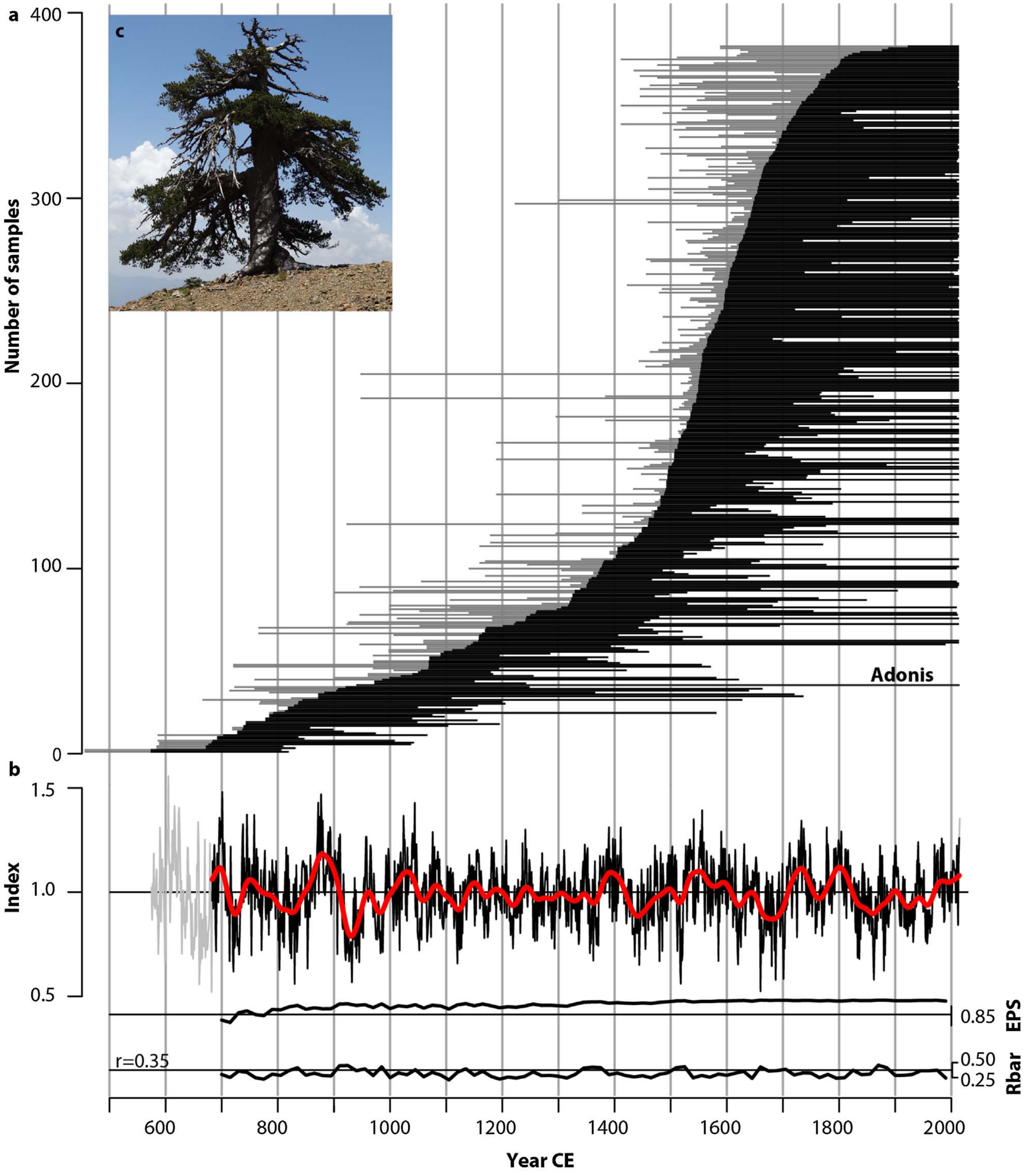

Fig. 2. Chronology characteristics: **a** temporal distribution of 382 core and disk samples encompassing 133017 measured tree rings from 4 sites. One bar represents an individual sample; the black section indicates the measured length and the grey section displays a pith-offset estimate; **b** power transformed 300 yr spline detrended Smolikas *Pinus heldreichii* TRW chronology (black, n < 5 grey) and corresponding 50 yr spline (red) with EPS and Rbar statistics computed for 30yr segments with 15 yrs of overlap in the bottom panels and **c** *Adonis*, a Bosnian pine, dendrochronologically dated to be 1075yrs. old and therefore currently the oldest living inhabitant in Europe. (For interpretation of the references to colour in this figure legend, the reader is referred to the web version of this article.)

differently exposed (NW, S, N, NE) sites on the eastern flanks and foothills of Mt. Smolikas (Fig. 2a). The climate in this elevation is characterized by hard, snowy winters with intense frost and snow melt occurring only in late spring. Summer dryness, typical for the Mediterranean climate, is reduced in northern Greece to less than three months (June to August). In addition to this, summer storms, which yield heavy rainfall, often moderate the hygrothermic summer conditions on Mt. Smolikas (Fotiadi et al., 1999; Loukas et al., 2002).

2.2. Chronology development, standardization and statistics

All disks and cores were prepared following standard dendrochronological techniques to produce fine-sanded surfaces for micrometer measurement (Strokes and Smiley, 1968). Tree-ring widths were measured in two labs by two different measuring systems; in Stockholm the Velmex System (Velmex Inc., Bloomfield, NY, USA) with and accuracy of 0.001 mm was used, and in Mainz the Lintab system with an accuracy of 0.01 mm was used (Rinn, 2003). Dating and measurement quality control was performed by skeleton plotting (Strokes and Smiley, 1968) and statistical cross-dating with the program COFECHA (Holmes, 1983). A data adaptive power transformation was applied to reduce the heteroscedastic structure of the TRW series (Büntgen et al., 2005; Cook and Peters, 1997) and the subsequent series standardized by calculating residuals from cubic smoothing splines with a 50% frequency-response cutoff at 300 years (Cook and Peters, 1981) using the software ARSTAN (Cook, 1985; Cook and Krusic, 2016). Based on the number of samples and the average correlation coefficients among the individual series (Rbar), variance stabilization was applied to all site chronologies (Frank et al., 2007). This standardization approach emphasizes inter-annual to multi-decadal variations, and minimizes centennial and longer trends (Cook et al., 1995). The final site TRW chronologies and composite TRW chronology were developed by calculating the robust bi-weight mean of tree-ring indices of each calendar year and truncated at the minimum sample size of < 5 series (Cook, 1985).

Growth and chronology characteristics were analyzed based on several statistical parameters using raw and standardized series. The running Rbar expresses the mean interseries correlation (Fritts, 1976) and the expressed population signal (EPS) describes the strength of the common variance within a chronology (Speer, 2010). A widely accepted level, indicating the reliability of the common signal, is 0.85. Both statistics were calculated for 30yr segments with 15yrs overlap. Average growth rates (AGR) were analyzed for the first 300yrs of living trees, which allows an inter-site growth comparison by reducing the influence of different age-structures. The establishment of regional curves (RC), empirically defined biological age/growth stand curves, permits further inter-site growth comparison (Briffa et al., 1992).

Climate-growth relationships were assessed using instrumental monthly and seasonal temperature and precipitation data from the Thessaloniki (40.52N/23.00E, 40 m a.s.l., Fig. 1c) and Larissa meteorological stations (39.62N/22.42E, 74 m a.s.l.). We recognize that the dryer and warmer climate in these eastern cities does not ideally represent the temperature and precipitation of the study site, however, the more proximal stations (e.g. Metsovo and Ioannina) could not be used for analysis due to their low data coverage. A spatial correlation analysis was computed between tree-ring chronologies and high-resolution 0.25° gridded E-OBS climate data (1950–2014 CE; Horvat et al., 1974) to explore the local and regional climate responses. All meteorological data were retrieved from the Royal Netherlands Meteorological Institute's (KNMI) Climate Explorer (https://climexp.knmi.nl; Trouet and Van Oldenborgh, 2013; van Oldenborgh, 2005).

High-frequency climate signal tests were performed to verify the strength of the tree-growth/climate relationship (Büntgen et al., 2008; Konter et al., 2015). A high-pass filter was applied by calculating the residuals between the standardized TRW, temperature, and precipitation time series and their corresponding 10-year cubic smoothing splines. Correlations between site chronologies and instrumental data were computed from the previous-year June to the current-year September, as well as for seasonal means of two, three, and four months (not all displayed). To test the climate signals' temporal stability, 31-year moving window correlations, between the maximum responding months or seasons and tree-ring indices, were calculated. Correlation maps were produced based on the original and first-differenced climate data to evaluate the spatial signal patterns at high and low frequencies.

3. Results

3.1. Intra- and inter-site growth characteristics

The Mt. Smolikas composite chronology contains annual to multi-decadal scale fluctuations (Fig. 2b). The number of single TRW measurement series integrated in this record changes considerably through time, from only ≤ 5 series in 683 CE to 31 series in 1000 CE, and 185 series in 2014 CE. Coherency among the individual TRW measurement series, expressed by the inter-series correlation, is moderate (mean Rbar = 0.35) but temporally robust, and indicates the potential of the Smolikas record for high-resolution climate reconstruction back to the first millennium. Mean chronology age calculated for each year over the period CE 575–2014 is fairly balanced prior to CE 1700, but increases towards the present, largely due to the integration of artificially younger remnant samples, a consequence of weathering, and consideration of samples from relatively old living trees. Biologically young trees, between 50 and 200 years, are underrepresented in the chronologies (Esper et al., 2016). Of the 15 cores with more than 700 rings, the longest is a living tree series containing 1075 rings, spanning the period 941–2015, and the longest relict series contained 865 rings, spanning the period 873–1737 (Fig. 2a). On multi-decadal scales, TRW index values increase during 920–1050, 1420–1540, 1650–1740 and 1850–2014, and decrease during 880–920, 1550–1690, and 1800–1850. The multi-decadal intervals of above-average growth characterizing the mid-16th century coincide with an increased regeneration, as many trees started growing in this period, likely indicating favorable climatic conditions (Fig. 2 b).

The lengths of site chronologies (n > 5 samples) range from 464 years at the N-exposed site to 1274 years at the NW-exposed site. Mean segment length varies between 296 years at the N- and 427 years at the NW-exposed site (Table 1). The site are robust (EPS ≥ 0.85) after 980 at the NW-exposed site, 1315 at the S-exposed site, 1610 at the N-exposed, and 1440 at the NE-exposed site. Trees at the NE-exposed site display the highest mean sensitivity, the highest Rbar, and the lowest average growth rate, which suggests a strong preservation of climatic information in high-frequency TRW variations. The opposite is true for

Table 1
Descriptive statistics of the four Mt. Smolikas site chronologies.

Site	Period CE	Chronology CE	MSL (yrs)	n trees	n cores	AGR	EPS (yrs)	AC[a]	SD[a]	MS[a]	Rbar[a]
NW	673–2014	740-2014	427	67	126	0.94	980	0.76	0.30	0.23	0.38
S	575–2014	1070-2014	316	57	111	0.75	1315	0.73	0.32	0.27	0.36
N	1425–2014	1550-2014	296	23	46	0.84	1610	0.73	0.32	0.22	0.33
NE	685–2014	1414-2014	308	47	99	0.70	1440	0.73	0.30	0.29	0.42
all	575–2014	683-2014	348	194	382	0.82	730	0.74	0.31	0.23	0.34

MSL: mean segment length, AGR: average growth rate of the first 300 years of growth from living trees, year until EPS is > 0.85, AC: first-order autocorrelation, SD: standard deviatio

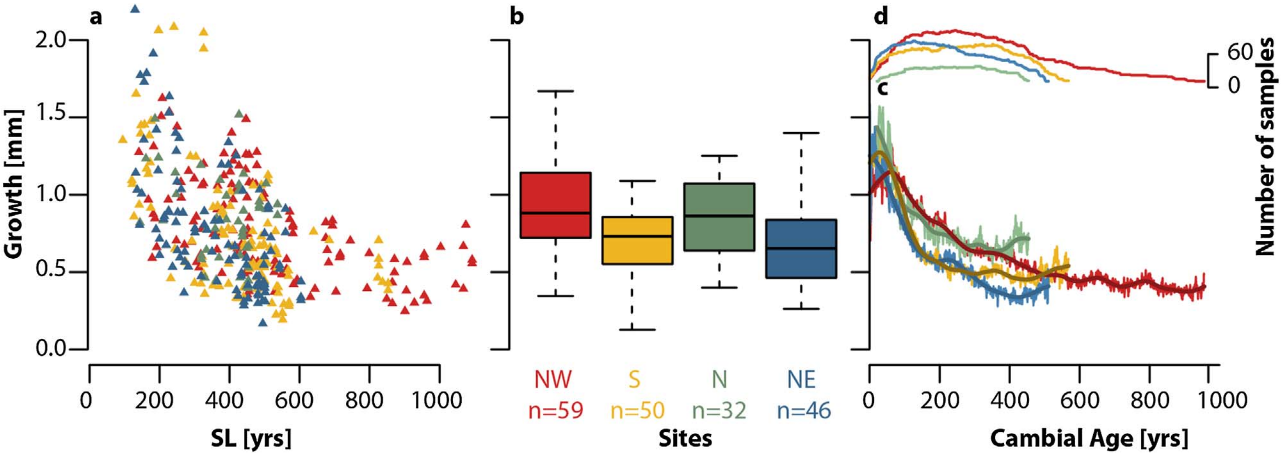

Fig. 3. Site-related growth characteristics: **a** growth rate to segment length (SL) ratio and **b** growth rates over the first 300yrs of living trees and **c** RCs (thin) and corresponding 100yr splines (bold) when n > 10 series and **d** number of samples incorporated in RCs.

trees at the N-exposed site, where the average growth rate is highest but the mean sensitivity and Rbar are lowest. In addition, moderate inter-site correlations ranging from r = 0.56 to 0.89 among the raw chronologies, and from r = 0.65 to r = 0.87 among the standardized chronologies over the 1550–2014 CE common period, point to substantial site-specific growth variations. The NW-, S- and N-exposed stands show an overall strong inter-site agreement, whereas their correspondence with the NE-exposed stand is surprisingly low.

The existence of heterogeneous growth rates, despite similar segment lengths, suggests there exists non-age-related inter- and intra-site differences (Fig. 3a). Biological growth rates for the first 300 years differ remarkably among sites despite the removal of remnant wood with uncertain pith-offset estimates (Fig. 3b). At the NW- and N-facing stands, the median and mean growth rates are significantly higher than at the S- and NE-facing stands. Intra-site variance of AGR is lower than inter-site variance, but single values largely overlap. The cambial age-alignment and subsequent averaging of the individual series to regional curves exhibits pronounced site differences, however (Fig. 3c). The regional curves have the same decreasing course through time, except for the first 150 years of growth at the NW-facing site, and the first 100 years of growth at the S-facing site. The absolute growth level differs at every point of cambial age, whereas it is persistently higher at the N- and NW- facing stands, and lower at the S- and NE- facing stands. The decline through time is a lifelong phenomenon and is still apparent after more than 800 years (Fig. 3c).

3.2. Climate signals

In the high-frequency domain (high-pass filtered data), tree growth at the four sites at Mt. Smolikas is significantly controlled by climate in April and June-July (Fig. 4). The climatic responses synchronize seasonally between the four sites: inter-site differences are relatively small compared to monthly and seasonal differences. At all sites, TRW is positively correlated with early summer (June-July) precipitation and negatively with early summer temperatures, whereas in spring (April) the signs are reversed. Previous years' precipitation and summer temperatures, as well as the current years' May, August, and September's climate, have no significant growth control. Though the relationships are not significant, temperatures in the previous years' autumn and winter are positively correlated with TRW.

Despite the synchronized growth/climate response pattern, some site-specific differences exist: The S-facing stand shows greatest response, and the NE-facing stand weakest response, to April temperatures ($r_{1931–2014} = 0.32–0.44$). These tendencies are reversed in June and July, when the S-facing stand shows the lowest and the NE-facing stand the highest response to June-July precipitation ($r_{1931–2014} = 0.28–0.45$). Precipitation in April ($r_{1931–2014} = -0.25–-0.38$) and temperature in June-July ($r_{1931–2014} = -0.18–-0.34$) are significantly anticorrelated with growth (Fig. 4a and c).

The post 1950 climate correlation coefficients are temporally stable (Fig. 4c–f). A period of relatively weak correlations prior to this date is followed by strengthened relationships; a systematic shift that occurs independently of the site and month. Splitting the 1931–2014 period into two equal sized windows, the correlation coefficient between April temperatures and the S-facing chronology improves from r = 0.37 to r = 0.49. Likewise, for June-July precipitation at the NE-facing site the correlations increase from r = 0.41 to r = 0.50. In addition, moving window correlations between average temperatures recorded at the stations in Thessaloniki and Larissa during the growing season, display an increasing synchronicity through time (Fig. 4g).

Spatial correlations between the site chronologies and E-OBS gridded June-July precipitation and April temperatures are weak, and little variance is explained by values from grids close to the study site (Fig. 5, insets). Correlation coefficients improve in the high-frequency domain, which underscores the strong growth/climate relationship at the inter-annual timescale. Positive significant correlation coefficients between TRW indices and June-July precipitation, and April temperatures are stable from central Italy, over large areas of the Balkan Peninsula, to the eastern Mediterranean (Fig. 5). Weaker, but still significant negative correlations occur over the British Isles, Spain, Scandinavia, Poland, and Ukraine. Even though all sites roughly share the same spatial temperature and precipitation patterns (only most diverse sites displayed in Fig. 5), site differences in spatial signal strength do occur. The S-exposed stand, with highest April temperature signal, is highly responsive to temperatures over large areas of the Balkan Peninsula but shows the least spatial connection to June-July precipitation. In contrast, the NE-exposed stand shows the weakest correlations with April temperatures, but the strongest correlations with June-July precipitation (Fig. 5).

4. Discussion

4.1. Evaluation of intra- and inter-site growth characteristics

The Smolikas *P. heldreichii* TRW compilation, dating back to CE 575, is potentially one of the most important natural-historical archives from the eastern Mediterranean due to its discrete provenance, length, and constantly high sample depth (n > 5 samples in CE 683). The living trees on Smolikas are exceptionally capable of producing a millennial-length chronology possessing a high degree of low-frequency climate variation (Esper et al., 2012; Esper et al., 2004). The most notable example is "Adonis" (Fig. 2c), a Bosnian pine that dendrochronologically

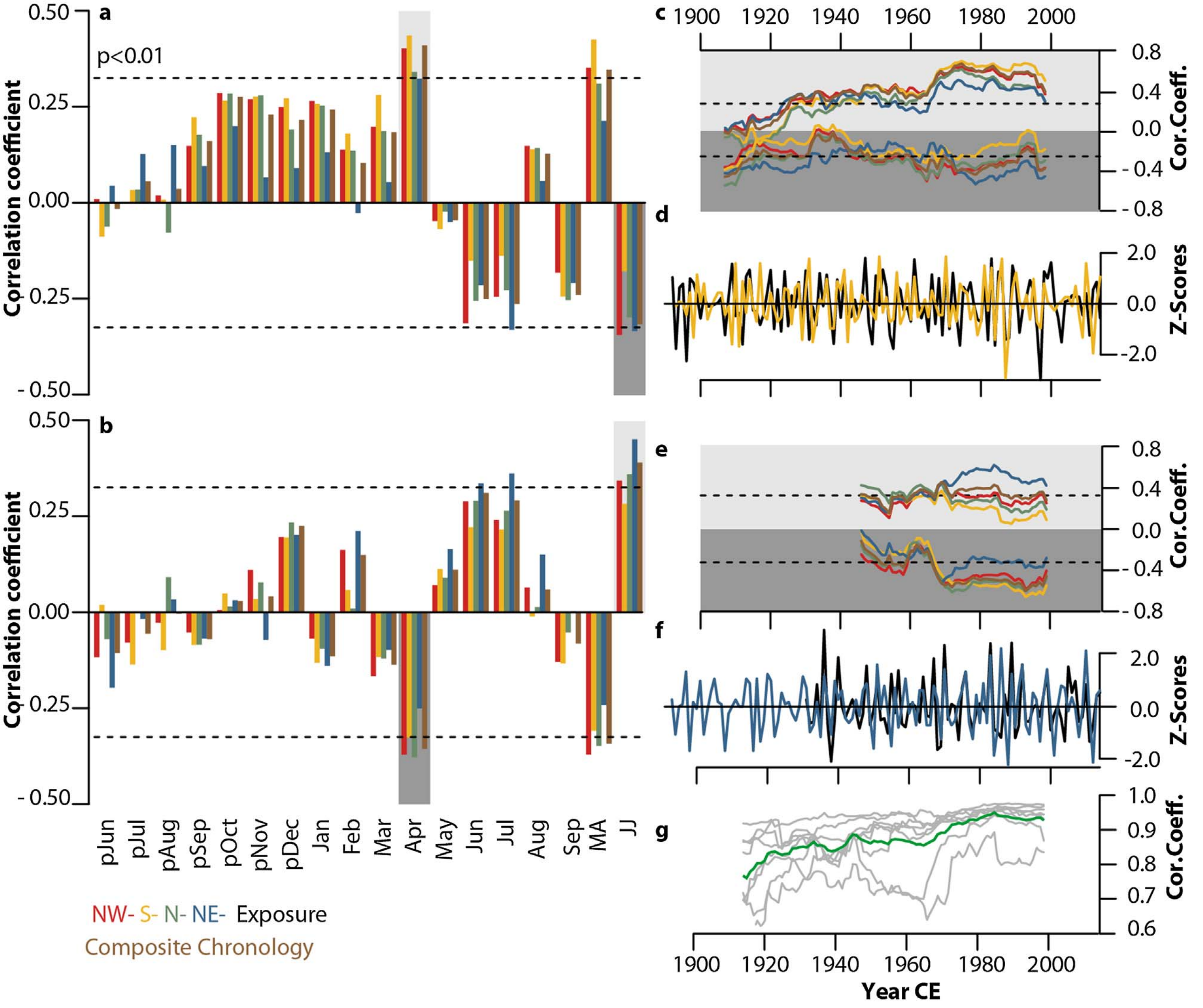

Fig. 4. Correlation coefficients of power transformed 300yr spline detrended and 10yr high-pass filtered site chronologies with 10yr high-pass filtered monthly **a** temperature and **b** precipitation data from the meteorological station in Thessaloniki (40.52N, 23.00E, 40m) for the period 1931–2014. Dashed lines indicate $p < 0.01$; 31 yr moving window correlations for the maximum responding month April and season June-July respectively for **c** temperature and **e** precipitation; Z-Scores of the maximum responding site chronology and **d** April temperatures (black) and **f** June-July precipitation (black); **g** 31yr moving window correlation coefficients between monthly temperature data (March to October, grey lines) from the meteorological stations in Thessaloniki and Larissa (39.63N, 22.42, 74m) and its mean (green). (For interpretation of the references to colour in this figure legend, the reader is referred to the web version of this article.)

dated to be over 1075 years old (Konter et al., 2017) making it the current, oldest known living tree in Europe providing a valuable history of past environmental conditions. Combining information from these living trees with remnant wood from the same site, we are able to extend the Smolikas chronology back in time with a high degree of sample replication.

Low inter-site correlations, the application of standardization techniques that stress different frequencies, and high site-specific Rbar values confirm the existence of site differences at multiple timescales (Düthorn et al., 2013). Young living trees between 50 and 200 years in age are underrepresented in our dataset, likely because agricultural activities throughout the 18th and 19th century have led to a reduced regeneration rate (Todaro et al., 2007). Due economic reasons the population decrease in the village Samarina, located at the foot of Mt. Smolikas, from 3000 inhabitants in 1890 to only 500 in 1960 (Beuermann, 1967), led to a reduction of free-range herd sizes. This supported a recovery of the forest stocks in the 20th and 21st centuries (McNeill, 1992). The absolute number of inhabitants in the region differs with the historical archive, but all reports note a remarkable decrease of population in the 20th century and subsequent reduction of grazing pressure (Beuermann, 1967; Brandes, 2007; McNeill, 1992).

Diverse growth levels and low inter-site correlations indicate substantial site differences. The wide range of growth rates between sites, despite identical ages, cannot be explained by age-effects alone. It is apparent that the differently exposed stands do not belong to the same biological growth population (Esper et al., 2003). The N- and NW- facing, versus the S- and NE-facing exposures are, respectively, the upper and lower range of growth extremes; the least growth-limited and least climatic-sensitive; and the most growth-limited and most climatic-sensitive (Fritts, 1976). In the NW-/S-facing stands the increase in growth over the first 150/100 years is related to biological forces. We find groups of trees standing relatively close together, competing for resources. Under such stand conditions the competitive power and growth rate of young trees is reduced (Chi et al., 2015). These findings suggest, that if applying RCS, the analysis of subsamples is highly recommended. Incorporating all series into a single Smolikas growth population might bias the resulting chronology and interpretation (Esper et al., 2003).

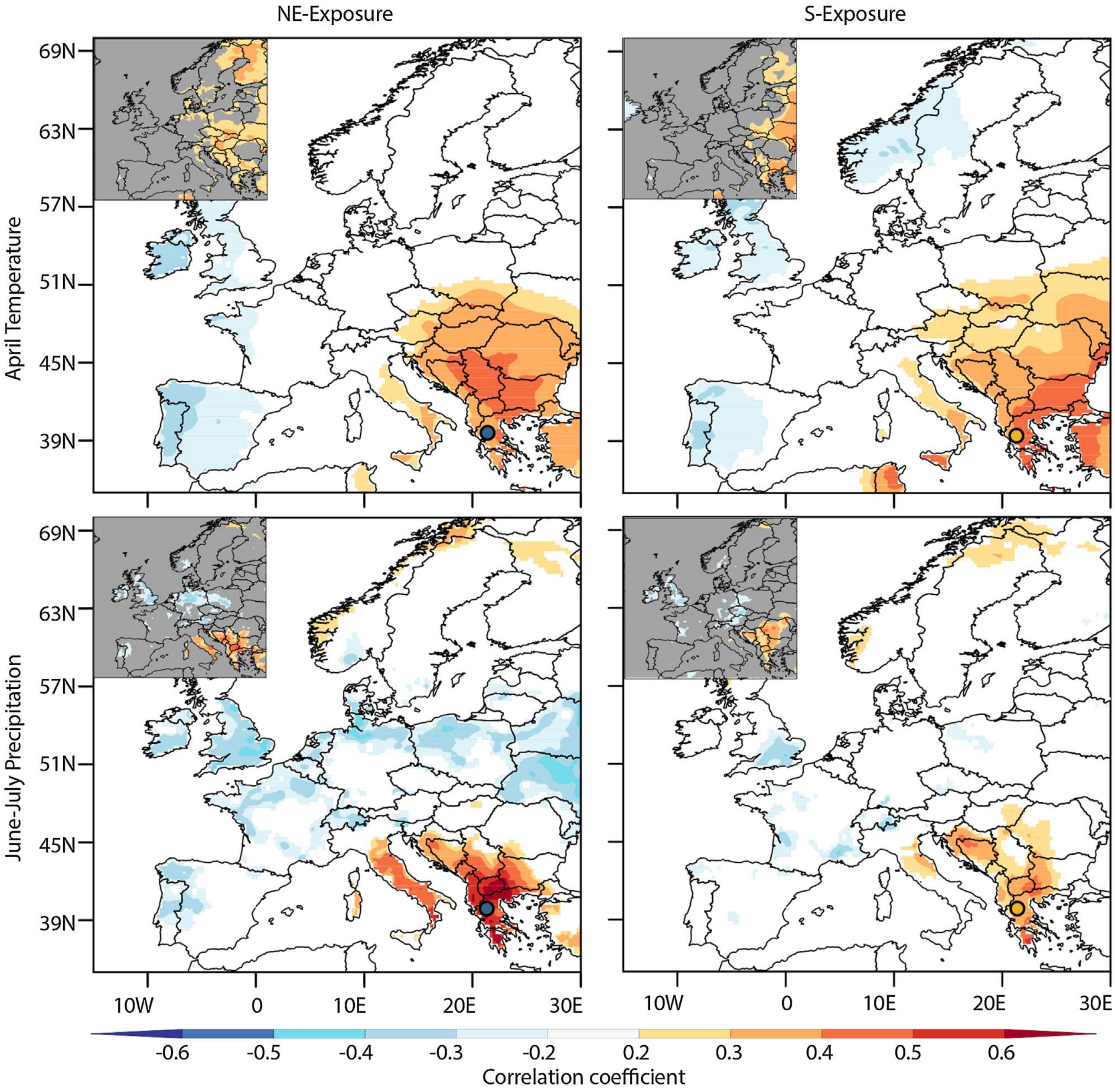

Fig. 5. Spatial correlations between gridded E-OBS 0.25° first differenced April temperature (upper panels) and June-July precipitation (lower panels) data with 300yr spline detrended chronologies of the NE-facing (left panels) and S-facing (right panels) stand when $p < 10\%$. Insets refer to original data and yellow and blue dots to the NE- and S-facing site respectively. (For interpretation of the references to colour in this figure legend, the reader is referred to the web version of this article.)

4.2. Climate signals

The seasonally uniform response of the differently exposed sites to temperature and precipitation demonstrates how the Mediterranean climate regime enforces growth synchronicity, whereas exposure only causes minor differences (Bolle, 2003; Loukas et al., 2002; Luterbacher et al., 2012; Seim et al., 2015). The site-independent positive shift in climate sensitivity post-1950s, and the temporally coinciding increase in station synchronicity of temperature data from Larissa and Thessaloniki, points to biases in the pre-1950 instrumental record. Caution must be exercised when considering these early data for calibration and reconstruction trials (Dienst et al., 2017; Mamara et al., 2012).

The inverse response between tree growth and April temperature (positive) and precipitation (negative) suggests dry and warm conditions favor growth in spring. These conditions enable a faster snowmelt and earlier start of cambial activity resulting in a longer growing season (Deslauriers et al., 2008). In contrast, high precipitation and colder temperatures affect a longer lasting snow cover, thereby delaying the onset of growth (Vaganov et al., 1999). The climate signal strength in April is associated with exposure effects: S-facing stands receive the strongest insolation and are most sensitive to April temperature. On the other hand, N- and NE-facing stands receive less solar radiation and are least sensitive to this parameter. A more intense and longer lasting daily insolation period on the S-facing slope enables larger warming and faster snowmelt, which in turn positively affects growth onset. N- and NE- facing slopes retain more moisture because lower insolation rates slow the thawing process (Holland and Steyn, 1975 Måren et al., 2015).

The positive association with previous autumn and winter temperatures, a period when the trees are dormant, has been found in previous studies (Panayotov et al., 2010; Trouet et al., 2012), but cannot be explained by cambial activity (Plomion et al., 2001). Cold and dry versus wet and warm conditions over southern Europe are associated with the strength of the North Atlantic Oscillation (Hurrell, 2003). During warm winters, snowfall is partially replaced by rainfall, resulting in a reduced snow pack and favoring an early growth onset (Vaganov et al., 1999). In addition to this, in warm winters the trees are less exposed to frost. Consequently, the likelihood of damage to roots and needles is reduced (Hartl-Meier et al., 2015; Panayotov et al., 2010; Tranquillini et al., 1979). In summer, drought stress, high temperatures, and water depletion induce a reduction of the metabolic and photosynthetic activity of trees that slows their growth (Chaves, 2002; Vieira et al., 2013). Anomalously wet and cool summers favor metabolic activity, whereas anomalously dry and warm summers increases drought stress and has the opposite effect (Levanic et al., 2013; Touchan et al., 2008).

Over a predominantly dry growing season, tree growth is simultaneously favored in spring and limited in summer. As a result, the absolute strength of the preserved climatic information in a tree ring is reduced. We suggest that the S-facing stand in particular shows a reduced response to summer precipitation because the stand greatly benefits from an early growth onset. The early start of the vegetation period enables the development of wide rings in spring (Rossi et al., 2007). The suggestion that early biomass gains may compensate losses by summer drought stress (Esper et al., 2007; Tejedor et al., 2015) cannot be properly defended as total ring-widths have only annual resolution (Fritts, 1976). By contrast those trees living in the NE-facing stand, without the benefit of early cell formation in spring, do capture a clear June-July climate signal. The N- and NE-facing stands are nearest to each other, yet display a different sensitivity to summer precipitation. The character of ground and surface meltwater flows effect on growth is one possible explanation. In the Mt. Smolikas sampling sites, the NW-, S- and N-facing slopes, meltwater likely infiltrates directly into the ground, thus making the trees less prone to summer droughts. On the NE-facing slope, water runoff through erosion channels causes fast depletion of poor soil water reserves. Such efficient drainage increases the tree's dependency on summer precipitation and drought exposure (King et al., 2013; Vieira et al., 2013).

The spatial correlation maps (Fig. 5) of gridded April temperature and June-July precipitation show strong climatic signals over the Balkan Peninsula related to common forcings, climate regimes, and synoptic patterns (Trouet, 2014; Trouet et al., 2012; Xoplaki et al., 2004; Xoplaki et al., 2012). The patterns are similar to those produced using the Thessaloniki climate data, underscoring the potential to reconstruct climate for different seasons and variables, using different site chronologies on Mt. Smolikas. The spatial correlation analysis also reveals a distinct dipole pattern across Europe that is consistent with the Summer North Atlantic Oscillation (sNAO) mode (Folland et al., 2009); responsible for annual and decadal summer temperature and drought variability over Greece (Oikonomou et al., 2010; Xoplaki et al., 2003). Temperature reconstructions using *P. heldreichii* MXD data from the Pirin Moutains in Bulgaria (Trouet et al., 2012) and Mt. Olympus in Greece (Klesse et al., 2015), are reported to have a strong and consistent anti-phase relationship with the sNAO (Folland et al., 2009), suggesting the sNAO is an important driver of the teleconnection between summer temperatures in northwestern versus southeastern Europe. In this analysis, we find some coherence with the sNAO, however, values are mostly insignificant. The weak sNAO signal is arguably related to the use of TRW which, compared to MXD, has a lower climatic signal strength, due to TRW's higher auto-correlation (Melvin et al., 2013).

In contrast to previous studies of *P. heldreichii* TRW data, that report climate signals of variable strength (Panayotov et al., 2010; Seim et al., 2012; Todaro et al., 2007), we find temporally robust signals after 1950. The significant and temporally robust April temperature correlations across all sites, and the statistically significant June-July precipitation signal in the NE-facing trees, suggests the TRW data from Mt. Smolikas have great potential for reconstructing climate. We hypothesize that the notable signal strength found, in comparison to previous *P. heldreichii* studies, is related to i) the standardization method used ii) slope exposure effects (Hartl-Meier et al., 2014; Hartl-Meier et al., 2015; Holland and Steyn, 1975), iii) higher site elevation with generally stronger growth limitations (Hartl-Meier et al., 2014 Körner, 2007), and iv) ecological effects including geomorphological modulated water supply (Fritts, 1976). Reduced signal strength, inherent to this and all previously mentioned studies, might be a consequence of the poorly representative meteorological station data used for analysis. Lowland station data tend to underestimate precipitation, and desiccation extremes at higher elevations (Fotiadi et al., 1999). The detection of distinct site differences in climate signal strength, on even small spatial scales, demonstrates the importance of careful site selection when performing dendroclimatological studies (Fritts, 1976).

5. Conclusion

We present an assessment of the site-specific climate signals in a new millennium-length TRW chronology from the Pindus Mountains of Greece that extends back to CE 575. We find inter-site differences in climate signal strength that appear to be related to slope exposure, biological memory effects, and meltwater supply. The strongest growth limitation is found at the S-facing site where trees are most sensitive to April temperatures, as well as at the NE-facing site where trees respond stronger to June-July precipitation. At the NW- and N-facing stands, *Pinus heldreichii* growth is least limited and contains a weaker climate signal. Due to opposing growth/climate relationships, manifest by warm and dry conditions supporting growth in spring but limiting growth in summer, biological memory effects arise and the initiation of cell formation in spring likely affects climate sensitivity in summer. If site differences are strictly considered, the climate of two seasons (April and June-July) could be reconstructed using only trees from S-exposed sites for temperature, and only trees from NE-exposed sites for precipitation. Further work will focus on (i) increasing sample replication through the inclusion of additional sites, (ii) investigating low-frequency trends in the millennial-length chronology, (iii) performing a TRW-based climate reconstruction, and (iv) producing MXD measurements to further explore the potential of reconstructing summer temperature variability in this Mediterranean environment.

Acknowledgements

Supported by the German Research Foundation (DFG, ES 161/9-1) and National Science Foundation CAREER grant (AGS-1349942). We are thankful to Soumaya Belmecheri, Tilmann Büttner, Manuel Dienst, Markus Kochbeck, Oliver Konter, Amarita Krusic, Anna Krusic, Jonas Krusic, Fredrik C. Ljungqvist, Sam Williams and Hakan Grudd for valuable assistance in the field.

References

Büntgen, U., Esper, J., Frank, D.C., Nicolussi, K., Schmidhalter, M., 2005. A 1052-year tree-ring proxy for Alpine summer temperatures. Clim. Dyn. 25, 141–153.

Büntgen, U., Frank, D., Wilson, R., Carrer, M., Urbinati, C., Esper, J., 2008. Testing for tree-ring divergence in the European Alps. Global Change Biol. 14, 2443–2453.

Büntgen, U., Tegel, W., Nicolussi, K., McCormick, M., Frank, D., Trouet, V., Kaplan, J.O., Herzig, F., Heussner, K.U., Wanner, H., Luterbacher, J., Esper, J., 2011. 2500 years of European climate variability and human susceptibility. Science 331, 578–582.

Beuermann, A., 1967. Fernweidewirtschaft in Südosteuropa: ein Beitrag zur Kulturgeographie des östlichen Mittelmeergebietes. Westermann, Braunschweig.

Bolle, H.-J., 2003. Mediterranean Climate. Springer Berlin Heidelberg, Berlin, Heidelberg.

Brandes, R., 2007. Waldgrenzen griechischer Hochgebirge: Unter besonderer Berücksichtigung des Taygetos, Südpeloponnes. Friedrich-Alexander-Universität Erlangen-Nürnberg.

Briffa, K.R., Jones, P.D., Bartholin, T.S., Eckstein, D., Schweingruber, F.H., Karlen, W., Zetterberg, P., Eronen, M., 1992. Fennoscandian summers from ad-500 − temperature-Changes on short and long timescales. Clim. Dyn. 7, 111–119.

Chaves, M.M., 2002. How plants cope with water stress in the field? photosynthesis and growth. Ann. Bot. 89, 907–916.

Chi, X.L., Tang, Z.Y., Xie, Z.Q., Guo, Q., Zhang, M., Ge, J.L., Xiong, G.M., Fang, J.Y., 2015. Effects of size, neighbors, and site condition on tree growth in a subtropical evergreen and deciduous broad-leaved mixed forest, China. Ecol. Evolution 5, 5149–5161.

Cook, E.R., Krusic, P.J., 2016. Program ARSTAN: a Tree-ring Standardization Program

Based on Detrending and Autoregressive Time Series Modeling, Wit Interactive Graphs., Lamont-Doherty Earth Observatory. Columbia University, Palisades NY.

Cook, E.R., Peters, K., 1981. The smoothing spline: a new approach to standardizing forest interior tree-ring width series for dendroclimatic studies. Tree-Ring Bull. 41.

Cook, E.R., Peters, K., 1997. Calculating unbiased tree-ring indices for the study of climatic and environmental change. Holocene 7, 361–370.

Cook, E., Briffa, K.R., Meko, D.M., Graybill, D., Funkhouser, G., 1995. The 'segment length curse' in long tree-ring chronology development for palaeoclimatic studies. The Holocene 229–237.

Cook, E.R., 1985. A Time Series Analysis Approach to Tree Ring Standardization.

Düthorn, E., Holzkämper, S., Timonen, M., Esper, J., 2013. Influence of micro-site conditions on tree-ring climate signals and trends in central and northern Sweden. Trees 27, 1395–1404.

D'Arrigo, R., Wilson, R., Jacoby, G., 2006. On the long-term context for late twentieth century warming. J. Geophys. Res. 111.

Deslauriers, A., Rossi, S., Anfodillo, T., Saracino, A., 2008. Cambial phenology, wood formation and temperature thresholds in two contrasting years at high altitude in southern Italy. Tree Physiol. 28, 863–871.

Dienst, M., Lindén, J., Engström, E., Esper, J., 2017. Removing the relocation bias from the 155-year Haparanda temperature record in Northern Europe. Int. J. Climatol.

Esper, J., Cook, E.R., Schweingruber, F.H., 2002. Low-frequency signals in long tree-ring chronologies for reconstructing past temperature variability. Science 295, 2250–2253.

Esper, J., Cook, E.R., Krusic, P.J., Peters, K., Schweingruber, F.H., 2003. Tests of the RCS method for preserving low-frequency variability in long tree-ring chronologies. Tree-Ring Res. 59, 81–98.

Esper, J., Treydte, K., Frank, D.C., Gärtner, H., Büntgen, U., 2004. Temperaturvariationen und Jahrringe | Temperature variation and tree rings. Schweizerische Zeitschrift fur Forstwesen 155, 213–221.

Esper, J., Frank, D., Büntgen, U., Verstege, A., Luterbacher, J., 2007. Long-term drought severity variations in Morocco. Geophys. Res. Lett. 34.

Esper, J., Buntgen, U., Timonen, M., Frank, D.C., 2012. Variability and extremes of northern Scandinavian summer temperatures over the past two millennia. Global Planet. Change 88-89, 1–9.

Esper, J., Krusic, P.J., Ljungqvist, F.C., Luterbacher, J., Carrer, M., Cook, E., Davi, N.K., Hartl-Meier, C., Kirdyanov, A., Konter, O., Myglan, V., Timonen, M., Treydte, K., Trouet, V., Villalba, R., Yang, B., Büntgen, U., 2016. Ranking of tree-ring based temperature reconstructions of the past millennium. Quat. Sci. Rev. 145, 134–151.

Folland, C.K., Knight, J., Linderholm, H.W., Fereday, D., Ineson, S., Hurrell, J.W., 2009. The summer north atlantic oscillation: past, present, and future. J. Clim. 22, 1082–1103.

Fotiadi, A.K., Metaxas, D.A., Bartzokas, A., 1999. A statistical study of precipitation in northwest Greece. Int. J. Climatol. 19, 1221–1232.

Frank, D., Esper, J., Cook, E.R., 2007. Adjustment for proxy number and coherence in a large-scale temperature reconstruction. Geophys. Res. Lett. 34.

Fritts, H.C., 1976. Tree Rings and Climate. Blackburn Press, Caldwell, N .J.

Gallardo-Cruz, J.A., Pérez-García, E.A., Meave, J.A., 2009. β-Diversity and vegetation structure as influenced by slope aspect and altitude in a seasonally dry tropical landscape. Landscape Ecol. 24, 473–482.

Hartl-Meier, C., Dittmar, C., Zang, C., Rothe, A., 2014. Mountain forest growth response to climate change in the Northern Limestone Alps. Trees-Struct. Funct. 28, 819–829.

Hartl-Meier, C., Zang, C., Buntgen, U., Esper, J., Rothe, A., Gottlein, A., Dirnbock, T., Treydte, K., 2015. Uniform climate sensitivity in tree-ring stable isotopes across species and sites in a mid-latitude temperate forest. Tree Physiol. 35, 4–15.

Holland, P.G., Steyn, D.G., 1975. Vegetational responses to latitudinal variations in slope angle and aspect. J. Biogeogr. 2, 179.

Holmes, R.L., 1983. Computer-assisted quality control in tree-ring dating and measurement. Tree-Ring Bull. 69–78.

Horvat, I., Glavač, V., Ellenberg, H., 1974. Vegetation Südosteuropas: Vegetation of Southeast-Europe. Fischer Stuttgart.

Hughes, P.D., Woodward, J.C., Gibbard, P.L., 2006. Late Pleistocene glaciers and climate in the Mediterranean. Global Planet. Change 50, 83–98.

Hurrell, J.W., 2003. The North Atlantic Oscillation: Climatic Significance and Environmental Impact, Geophysical Monograph. American Geophysical Union, Washington, DC, pp. 279.

Körner, C., 2007. The use of 'altitude' in ecological research. Trends Ecol. Evol. 22, 569–574.

Köse, N., Akkemik Ü, Dalfes, H.N., Özeren, M.S., 2011. Tree-ring reconstructions of May?June precipitation for western Anatolia. Quat. Res. 75, 438–450.

King, G., Fonti, P., Nievergelt, D., Buntgen, U., Frank, D., 2013. Climatic drivers of hourly to yearly tree radius variations along a 6 degrees C natural warming gradient. Agric. Forest Meteorol. 168, 36–46.

Klesse, S., Ziehmer, M., Rousakis, G., Trouet, V., Frank, D., 2015. Synoptic drivers of 400 years of summer temperature and precipitation variability on Mt. Olympus, Greece. Clim. Dyn. 45, 807–824.

Konter, O., Rosner, K., Kyncl Thomas Esper, J., Büntgen, U., 2015. Spatiotemporal variations in the climatic response of Larix decidua from the Slovakian Tatra Mountains. Wilson, R., Helle, G., Gaertner, H. (Eds.), Proceedings of the DENDROSYMPOSIUM 2014. Deutsches GeoForschungsZentrum GFZ 62–69.

Konter, O., Krusic, P.J., Trouet, V., Esper, J., 2017. Meet Adonis, Europe's oldest dendrochronologically dated tree. Dendrochronologia 42, 12.

Kovats, R.S., Valentini, R., Bouwer, L.M., Georgopoulou, E., Jacob, D., Martin, E., Rounsevell, M., Soussana, J.-F., 2014. Europe. In: Barros, V.R., Field, C.B., Dokken, D.J., Mastrandrea, M.D., MacH, K.J., Bilir, T.E., Chatterjee, M., Ebi, K.L., Estrada, Y.O., Genova, R.C., Girma, B., Kissel, E.S., Levy, A.N., MacCracken, S., Mastrandrea, P.R., White, L.L. (Eds.), Climate Change 2014: Impacts, Adaptation, and Vulnerability. Part B: Regional Aspects. Contribution of Working Group II to the Fifth Assessment Report of the Intergovernmental Panel of Climate Change. Cambridge University Press Cambridge, United Kingdom and New York, NY USA, pp. 1267–1326.

Levanic, T., Popa, I., Poljansek, S., Nechita, C., 2013. A 323-year long reconstruction of drought for SW Romania based on black pine (Pinus Nigra) tree-ring widths. Int. J. Biometeorol. 57, 703–714.

Loukas, A., Vasiliades, L., Dalezios, N.R., 2002. Hydroclimatic variability of regional droughts in Greece using the palmer moisture anomaly index. Nord Hydrol. 33, 425–442.

Luterbacher, J., García-Herrera, R., Akcer-On, S., Allan, R., Alvarez-Castro, M.-C., Benito, G., Booth, J., Büntgen, U., Cagatay, N., Colombaroli, D., Davis, B., Esper, J., Felis, T., Fleitmann, D., Frank, D., Gallego, D., Garcia-Bustamante, E., Glaser, R., Gonzalez-Rouco, F.J., Goosse, H., Kiefer, T., Macklin, M.G., Manning, S.W., Montagna, P., Newman, L., Power, M.J., Rath, V., Ribera, P., Riemann, D., Roberts, N., Sicre, M.-A., Silenzi, S., Tinner, W., Tzedakis, P.C., Valero-Garcés, B., van der Schrier, G., Vannière, B., Vogt, S., Wanner, H., Werner, J.P., Willett, G., Williams, M.H., Xoplaki, E., Zerefos, C.S., Zorita, E., 2012. A review of 2000 years of paleoclimatic evidence in the mediterranean. In: Lionello, P. (Ed.), The Climate of the Mediterranean Region, 1. ed. ed. Elsevier Science, Amsterdam, pp. 87–185.

Måren, I.E., Karki, S., Prajapati, C., Yadav, R.K., Shrestha, B.B., 2015. Facing north or south: does slope aspect impact forest stand characteristics and soil properties in a semiarid trans-Himalayan valley? J. Arid Environ. 121, 112–123.

Mamara, A., Argiriou, A.A., Anadranistakis, M., 2012. Homogenization of mean monthly temperature time series of Greece. Int. J. Climatol.

McNeill, J.R., 1992. The Mountains of the Mediterranean World: An Environmental History. Cambridge Univ. Press, Cambridge.

Meiggs, R., 1982. Trees and Timber in the Ancient Mediterranean World. Clarendon Pr, Oxford.

Melvin, T.M., Grudd, H., Briffa, K.R., 2013. Potential bias in 'updating' tree-ring chronologies using regional curve standardisation: re-processing 1500 years of Tornetrask density and ring-width data. The Holocene 23, 364–373.

Oikonomou, C., Flocas, H.A., Hatzaki, M., Nisantzi, A., Asimakopoulos, D.N., 2010. Relationship of extreme dry spells in Eastern Mediterranean with large-scale circulation. Theor. Appl. Climatol. 100, 137–151.

Panayotov, M., Bebi, P., Trouet, V., Yurukov, S., 2010. Climate signal in tree-ring chronologies of Pinus peuce and Pinus heldreichii from the Pirin Mountains in Bulgaria. Trees-Struct Funct 24, 479–490.

Paudel, S., Vetaas, O.R., 2014. Effects of topography and land use on woody plant species composition and beta diversity in an arid Trans-Himalayan landscape, Nepal. Journal of Mountain Science 11, 1112–1122.

Plomion, C., Leprovost, G., Stokes, A., 2001. Wood formation in trees. Plant Physiol. 127, 1513–1523.

Pook, E., Moore, C., 1966. The influence of aspect on the composition and structureof dry sclerophyll forest on black mountain Canberra. ACT. Aust. J. Bot. 14, 223–242.

Rinn, F., 2003. Time Series Analysis and Presentation for Dendrochronologyand Related Applications. Heidelberg.

Rossi, S., Deslauriers, A., Anfodillo, T., Carraro, V., 2007. Evidence of threshold temperatures for xylogenesis in conifers at high altitudes. Oecologia 152, 1–12.

Schneider, L., Smerdon, J.E., Büntgen, U., Wilson, R.J.S., Myglan, V.S., Kirdyanov, A.V., Esper, J., 2015. Revising midlatitude summer temperatures back to A.D. 600 based on a wood density network. Geophys. Res. Lett. 42, 4556–4562.

Schweingruber, F.H., 1996. Tree Rings and Environment Dendroecology. Haupt, Berne, Stuttgart, Vienna.

Seftigen, K., Linderholm, H.W., Drobyshev, I., Niklasson, M., 2013. Reconstructed drought variability in southeastern Sweden since the 1650. Int. J. Climatol. 33, 2449–2458.

Seim, A., Buntgen, U., Fonti, P., Haska, H., Herzig, F., Tegel, W., Trouet, V., Treydte, K., 2012. Climate sensitivity of a millennium-long pine chronology from Albania. Climate Res. 51, 217–228.

Seim, A., Treydte, K., Trouet, V., Frank, D., Fonti, P., Tegel, W., Panayotov, M., Fernandez-Donado, L., Krusic, P., Buntgen, U., 2015. Climate sensitivity of Mediterranean pine growth reveals distinct east-west dipole. Int. J. Climatol. 35, 2503–2513.

Speer, J.H., 2010. Fundamentals of Tree-ring Research. Univ. of Arizona Press Tucson, Ariz.

Sternberg, M., Shoshany, M., 2001. Influence of slope aspect on Mediterranean woody formations: comparison of a semiarid and an arid site in Israel. Ecol. Res. 16, 335–345.

Stevanovic, V., Tan, K., Iatrou, G., 2003. Distribution of the endemic Balkan flora on serpentine − I. obligate serpentine endemics. Plant Systematics Evolut. 242, 149–170.

Stoffel, M., Khodri, M., Corona, C., Guillet, S., Poulain, V., Bekki, S., Guiot, J., Luckman, B.H., Oppenheimer, C., Lebas, N., Beniston, M., Masson-Delmotte, V., 2015. Estimates of volcanic-induced cooling in the Northern Hemisphere over the past 1,500 years. Nat. Geosci. 8, 784-+.

Strokes, M.A., Smiley, T.L., 1968. An Introduction to Tree Ring Dating. The University of Chicargo Press, Chigargo, USA.

Tejedor, E., de Luis, M., Cuadrat, J.M., Esper, J., Saz, M.A., 2016. Tree-ring-based drought reconstruction in the iberian range (east of Spain) since 1694. Int. J. Biometeorol. 361–372.

Todaro, L., Andreu, L., D'Alessandro, C.M., Gutirrez, E., Cherubinic, P., Saracino, A., 2007. Response of Pinus leucodermis to climate and anthropogenic activity in the National Park of Pollino (Basilicata, Southern Italy). Biol. Conserv. 137, 507–519.

Touchan, R., Meko, D.M., Aloui, A., 2008. Precipitation reconstruction for Northwestern Tunisia from tree rings. J. Arid Environ. 72, 1887–1896.

Tranquillini, W., Billings, W.D., Golley, F., Lange, O.L., Olson, J.S., 1979. Physiological Ecology of the Alpine Timberline. Springer Berlin Heidelberg, Berlin, Heidelberg.

Trouet, V., Van Oldenborgh, G.J., 2013. KNMI climate explorer: a web-Based research tool for high-Resolution paleoclimatology. Tree-Ring Res. 69, 3–13.

Trouet, V., Panayotov, M.P., Ivanova, A., Frank, D., 2012. A pan-European summer teleconnection mode recorded by a new temperature reconstruction from the northeastern Mediterranean (1768 CE-2008). Holocene 22, 887–898.

Trouet, V., 2014. A tree-Ring based late summer temperature reconstruction (1675 CE-1980) for the northeastern mediterranean. Radiocarbon 56, S69–S78.

Urban, D.L., Miller, C., Halpin, P.N., Stephenson, N.L., 2000. Forest gradient response in Sierran landscapes: the physical template. Landscape Ecol. 15, 603–620.

Vaganov, E.A., Hughes, M.K., Kirdyanov, A.V., Schweingruber, F.H., Silkin, P.P., 1999. Influence of snowfall and melt timing on tree growth in subarctic Eurasia. Nature 400, 149–151.

Vieira, J., Rossi, S., Campelo, F., Freitas, H., Nabais, C., 2013. Seasonal and daily cycles of stem radial variation of Pinus pinaster in a drought-prone environment. Agric. Forest Meteorol. 180, 173–181.

Wilson, R., Anchukaitis, K., Briffa, K.R., Büntgen, U., Cook, E., D'Arrigo, R., Davi, N., Esper, J., Frank, D., Gunnarson, B., Hegerl, G., Helama, S., Klesse, S., Krusic, P.J., Linderholm, H.W., Myglan, V., Osborn, T.J., Rydval, M., Schneider, L., Schurer, A., Wiles, G., Zhang, P., Zorita, E., 2016. Last millennium northern hemisphere summer temperatures from tree rings: part I: The long term context. Quat. Sci. Rev. 134, 1–18.

Xoplaki, E., Gonzalez-Rouco, J.F., Gyalistras, D., Luterbacher, J., Rickli, R., Wanner, H., 2003. Interannual summer air temperature variability over Greece and its connection to the large-scale atmospheric circulation and Mediterranean SSTs 1950–1999. Clim. Dyn. 20, 537–554.

Xoplaki, E., Gonzalez-Rouco, J.F., Luterbacher, J., Wanner, H., 2004. Wet season Mediterranean precipitation variability: influence of large-scale dynamics and trends. Clim. Dyn. 23, 63–78.

van Oldenborgh, G.J., 2005. Searching for decadal variations in ENSO precipitation teleconnections. Geophys. Res. Lett. 32.

Xoplaki, E., Trigo, R.M., García-Herrera, R., Barriopedro, D., D'Andrea, F., Fischer, E.M., Gimeno, L., Gouveia, C., Hernández, E., Kuglitsch, F.G., Mariotti, A., Nieto, R., Pinto, J.G., Pozo-Vázquez, D., Saaroni, H., Toreti, A., Trigo, I.F., Vicente-Serrano, S.M., Yiou, P., Ziv, B., 2012. Large-Scale Atmospheric Circulation Driving Extreme Climate Events in the Mediterranean and Its Related Impacts, The Climate of the Mediterranean Region. Elsevierpp. 347–417.